Composites: Part B 43 (2012) 3507–3515

Contents lists available at SciVerse ScienceDirect

Composites: Part B

journal homepage: www.elsevier.com/locate/compositesb

# Covalent and non-covalent functionalized MWCNTs for improved thermo-mechanical properties of epoxy composites

C.M. Damian, S.A. Garea, E. Vasile, H. Iovu *

*Advanced Polymer Materials Group, University Politehnica of Bucharest, Faculty of Applied Chemistry and Materials Science, Calea Victoriei 149, Bucharest 010072, Romania*

ARTICLE INFO

*Article history:*
Received 22 September 2011
Received in revised form 10 November 2011
Accepted 30 November 2011
Available online 20 December 2011

*Keywords:*
A. Nano-structures
A. Polymer–matrix composites (PMCs)
D. Thermal analysis
D. Electron microscopy

ABSTRACT

Two simplified methods for non-covalent and covalent functionalization of multiwalled carbon nanotubes (MWCNTs) with surfactants were developed, the functionalization degree and properties of their epoxy nanocomposites were studied. Physical absorption and covalent attachment of nonionic surfactants was proved by an increase of the mass loss in TGA and the appearance of characteristic peaks in XPS. The DSC analysis of the epoxy nanocomposites proved a low catalytic influence of 1% modified MWCNTs on the epoxy curing process, while DMA showed a higher flexibility compared with the neat epoxy. Dispersion state of modified MWCNTs in epoxy was related to their functionalization degree.



## 1. Introduction

Carbon nanotubes (CNTs) are widely studied materials, due to their excellent thermal [1] and physical properties [2]. They are expected to give novel applications in electrochemical sensors [3,4], or different types of composites or solutions [5,6].

The high aspect ratio of the CNTs results in strong van der Waals attraction forces between individual nanotubes, as a result they exist mainly in bundles. Their full potential in property improvement can be achieved only if they have a good adhesion to the polymer matrix [7–9] of the composites leading to a well-dispersed reinforcing agent.

The reinforcement effect of CNTs in the composites depends not only on their concentration within the hosting system but also on the level of dispersion. Having individually dispersed CNTs in polymer systems and reaching a strong interface between them is a challenging task to obtain new light weight nanocomposite materials with improved mechanical properties [10], electrical or thermal conductivity [11], while usually the polymer materials are non-conductive. Improvements in thermal properties could have applications in thermal coating systems for dissipating heat from electronics. Mechanical properties improvement mechanism of CNTs could be to bridge between the crack faces of the composite to retard the crack propagation process allowing the materials to be used in applications where reduced weight and increased strength are needed such as in the aerospace industry [12].

The CNT–polymer interface adhesion is generally improved by a surface modification of the nanotubes trough functionalization which may be either covalent [13–15] or non-covalent methods [16,17]. A covalent surface functionalization is effective in improving the adhesion and chemical properties of the composites but it exhibits the disadvantage of disturbing to some extent the graphitic structure of CNT walls [18,19]. Typical non-covalent functionalization methods may improve both modulus and strength of the composites [20,21] while the nanotubes graphitic structure and properties are maintained at the initial values. The use of surfactant molecules to change the surface energy of the nanotubes avoids the aggressive chemical functionalization which may destroy the π electronic system of the sidewall graphene structure. The hydrophobic part of the surfactant is oriented towards the surface of the carbon nanotubes, whereas the polar part interacts in the outer region with the solvent molecules.

Different types of surfactants like sodium dodecyl sulfate (SDS), polyethylene glycol sorbitan (Tween series) or hexadecyl trimethyl ammonium bromide (CTAB) were studied as dispersion supports for MWCNTs by several research groups [21–25]. While the previously developed methods used relatively high concentration of surfactants, our work focused on utilizing just the surfactant molecules absorbed at the MWCNTs surface.

The goal of this work was to improve the dispersion of MWCNTs within the epoxy polymer through non-covalent and covalent functionalization of their graphitic sidewalls and to improve the thermo-mechanical properties of the final epoxy composites.

* Corresponding author. Tel.: +40 214023922; fax: +40 213111796.
*E-mail address:* iovu@tsocm.pub.ro (H. Iovu).

1359-8368/$ - see front matter © 2011 Elsevier Ltd. All rights reserved.
doi:10.1016/j.compositesb.2011.11.052

## 2. Experimental

### 2.1. Materials

Multiwalled carbon nanotubes were supplied by Aldrich being produced by Catalytic Chemical Vapor Deposition (CCVD) with more than 90% carbon basis.

Three types of nonionic surfactants received from Aldrich were used: octylphenoxypolyethoxyethanol (Triton X100) (HLB = 13.5), alkyl polyethylene glycol (Triton SP-135) (HLB = 8), alkylphenyl-polyethylene glycol (Tergitol NP-9) (HLB = 12.9).

The solvent used was acetone purchased from Aldrich.

### 2.2. Characterization

Thermogravimetric Analysis (TGA) curves were registered on a Q500 TA Instruments equipment, under nitrogen atmosphere using a heating rate of 10 °C/min from room temperature to 800 °C.

Raman Spectroscopy was done on a DXR Raman Microscope from Thermo Scientific using a 633 nm laser with a maximum laser power of 14 mW. The laser beam was focused with the 10× objective.

The surface structures for different types of MWCNTs were studied by X-ray Photoelectron Spectroscopy (XPS) using a K-Alpha instrument from Thermo Scientific, with a monochromated Al $K_\alpha$ source (1486.6 eV), at a bass pressure of $2 \times 10^{-9}$ mbar. Charging effects were compensated by a flood gun and binding energies were calibrated by placing the C 1s peak at 284.6 eV as internal standard. The pass energy for the survey spectra was 200 eV and 20 eV for high resolution. Deconvolutions of the C 1s, O 1s peaks were performed after Shirley's inelastic background subtraction and were normalized for the measured transmission function of the spectrometer.

Transmission Electron Microscopy (TEM) images were achieved on a Tecnai G2 F30 S-TWIN equipment provided with a 200 kV acceleration voltage emission gun. Ultra thin sections of composites having 50 nm thicknesses were cut with Leica Ultracut UCT ultramicrotome equipped with a diamond knife.

Differential Scanning Calorimetry (DSC) curves were recorded on a Netzsch DSC 204 F1 Phoenix equipment. The sample was heated from RT to 300 °C using a heating rate of 10 °C/min under nitrogen (20 mL/min flow rate).

Dynamic-Mechanical Analysis (DMA) tests were done on a TRITEC 2000 B equipment. Samples were analyzed in single cantilever bending mode at 1 Hz frequency. Data were collected from RT to 180 °C using a heating rate of 5 °C/min.

Mechanical Tests: compressive tests were performed on a Universal Testing Machine Instron 3382 with 100 kN load-cell at room temperature. The cylinder type samples with 10–11 mm thickness and 10–11 mm diameter were placed on the lower plate and compressed by the upper plate at a constant compression rate of 5 mm/min until fragmentation occurred. Measurements were done 5–6 times for each sample and the average value was reported.

Scanning electron microscopy (SEM) was done on a Quanta Inspect F (FEI) instrument, with field emission electron gun, 1.2 nm resolution and X-ray energy dispersive spectrometer having an accelerating voltage of 30 kV. For a better contrast, the samples were first fractured in liquid nitrogen and covered with a thin gold layer.

### 2.3. MWCNTs functionalization

(a) non-covalent functionalization was done by using a 1 vol%. solution of surfactant in acetone. The amounts of MWCNTs were calculated to obtain a suspension of 1.25 mg/mL concentration in acetone-surfactant solution. The mixture was kept in the ultrasound bath at room temperature for 6 h in order to disperse nanotubes individually and to obtain physically absorbed surfactant molecules on the MWCNTs sidewalls as shown in Fig. 1. The suspension was filtered on a PTFE membrane with 0.22 μm pores and washed several times with acetone to remove unattached molecules which could affect the thermo-mechanical properties of the subsequent composites. The obtained functionalized CNTs were dried under vacuum for 24 h at RT and further thermally and structurally characterized.

(b) The second method to obtain functionalized CNTs was a two step process consisting in oxidizing first the MWCNTs followed by an esterification reaction according to an adapted method described in the literature [26]. Thus 100 mg of MWCNTs were oxidized with 3:1 vol. sulfuric and nitric acid mixture by refluxing at 70 °C. This procedure creates carboxylic defects in their graphitic structure [19]. The obtained MWCNT-COOH were washed and dried in vacuum. Then they react with the hydroxyl groups from the surfactants in acid medium (pH = 2) as shown in Fig. 2.

### 2.4. Synthesis of the epoxy composites

Calculated amounts of unmodified and functionalized MWCNTs (1 wt.%) were mixed with diglycidylether of bisphenol A (DGEBA). The mixture was then sonicated using a Hielscher UP100H sonicator for 2 h having 60% amplitude at room temperature. Then the hardener was added to the mixture and vigorously stirred for 2 min. Air bubbles were removed by placing the mixture in an ultrasound bath with degas function for 2 min. The bubble free mixture was then cast into a mold and cured at 60 °C for 3 h followed by 1 h postcuring process at 100 °C.

## 3. Results and discussion

### 3.1. Functionalized MWCNTs characterization

Isolation of individual nanotubes from a bundle by surfactant absorption was achieved by propagation of the spaces or gaps formed at the bundle ends through sonication. The surfactant absorption is preventing the re-agglomeration and is enlarging the spaces between MWCNTs, ultimately separating the individual nanotubes from the bundle. TGA curves of non-covalently functionalized MWCNTs shown in Fig. 3a are the first indication that surfactant molecules were absorbed on MWCNT surface. Thus compared with unmodified MWCNTs one can observe that the mass loss of functionalized MWCNTs increased due to the lower stability of the organic modifier molecules. This process also depends on the surfactant concentration attached onto the MWCNTs surface. The functionalized MWCNTs degradation occurs in two steps: the first step in the range 200–500 °C being assigned to the degradation of the molecules attached to MWCNT surface as it is shown by the DTG curves (Fig. 3b), and the second step which starts from 500 °C and goes to temperatures above 900 °C corresponding to the thermal-oxidative degradation due to the thermal decomposition of the disordered carbon. The unmodified MWCNTs show a plateau of the curve up to 500 °C, the temperature at which the thermal-oxidative degradation starts.

The TGA curves for the covalently functionalized MWCNTs are compared with that of MWCNT-COOH in Fig. 4, showing a low increase in the mass loss for SP135 and X100 but a significant increase for the MWCNTs modified with NP9, this difference being attributed to a higher number of surfactant molecules attached to the nanotubes walls for the same surfactant concentration used.

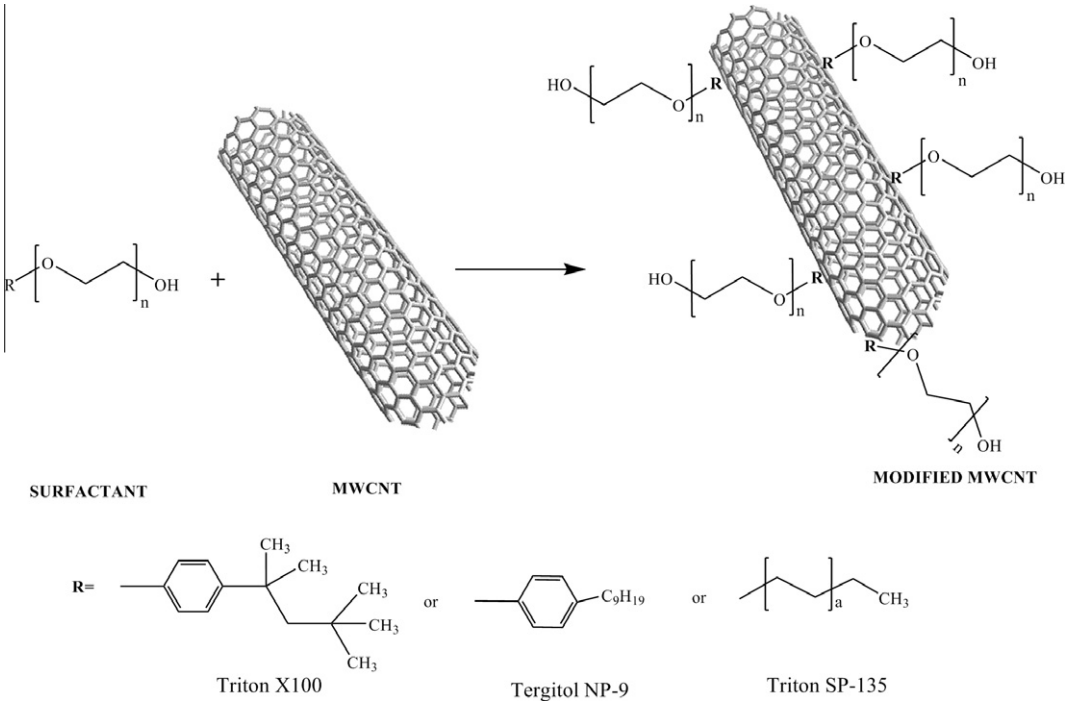


**Fig. 1.** Surface absorption of surfactant molecules on MWCNTs.

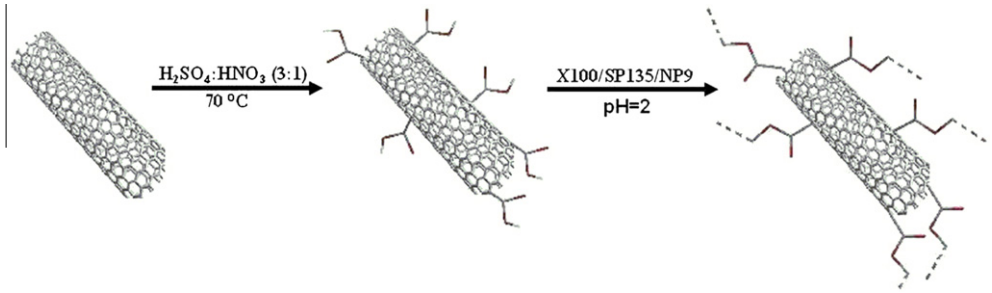


**Fig. 2.** Covalent functionalization of MWCNTs with surfactants.

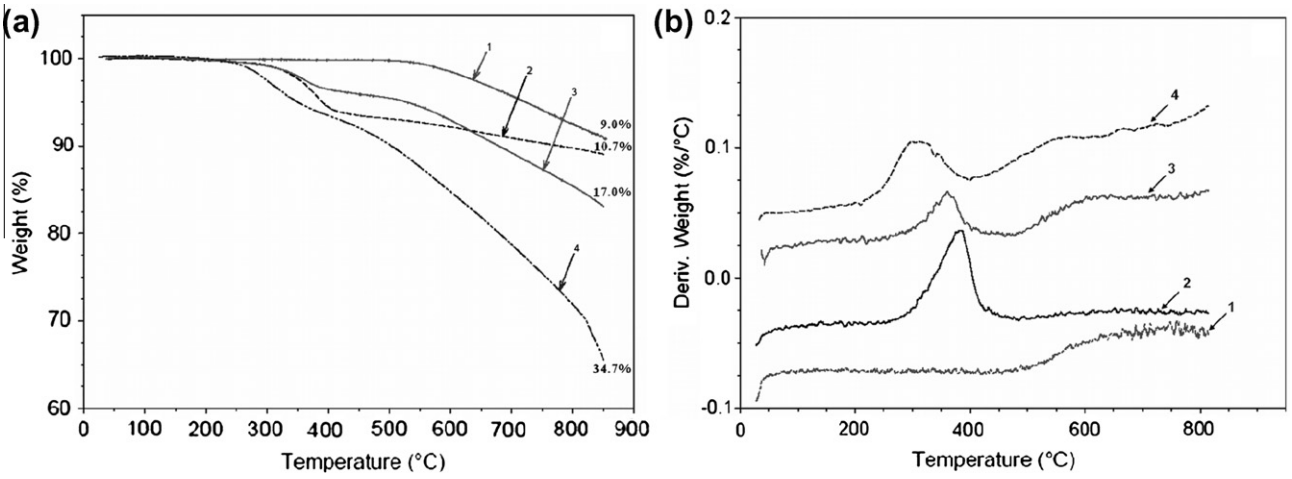


**Fig. 3.** TGA (a) and DTG (b) curves for non-covalent functionalized MWCNTs: (1) MWCNT, (2) MWCNT-X100, (3) MWCNT-SP135, and (4) MWCNT-NP9.

Comparing the TGA curves after covalent functionalization with those registered after non-covalent procedure, one may observe that the mass losses are always higher for covalent method because covalent functionalization is accompanied by non-covalent attachment of surfactants molecules to some extent. Moreover the DTG curves (Fig. 4b) show that especially for NP9

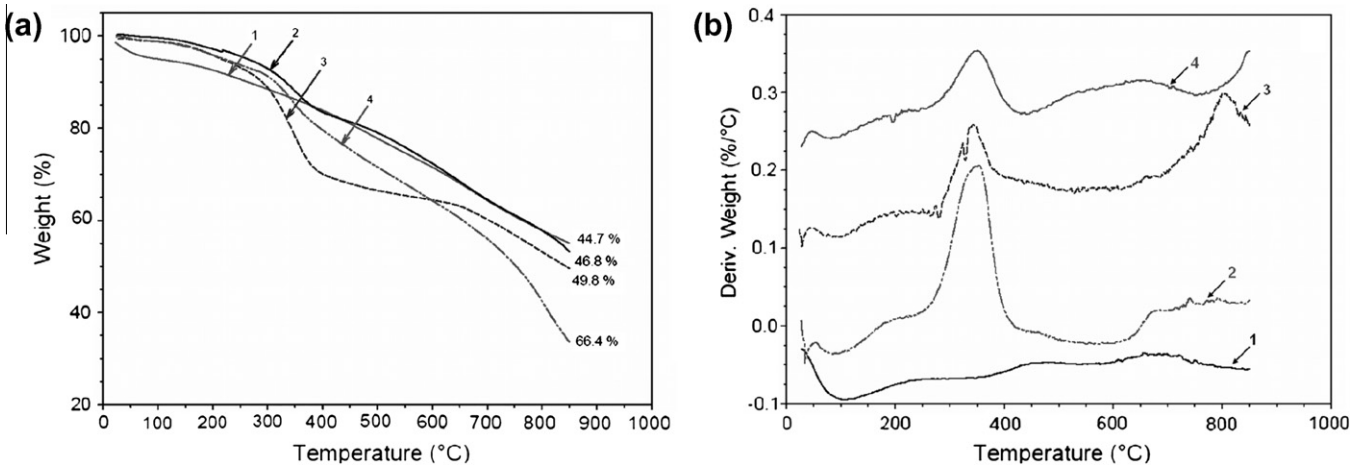


**Fig. 4.** TGA (a) and DTG (b) curves for covalent functionalized MWCNTs: (1) MWCNT-COOH, (2) MWCNT-COO-X100, (3) MWCNT-COO-SP135, and (4) MWCNT-COO-NP9.

the temperature corresponding to the maximum degradation rate is higher for the covalent method in comparison with the non-covalent ones due to the stronger covalent bonds formed between the NP9 molecules and MWCNTs surface.

The Raman spectra (Fig. 5) show two significant peaks, one at 1593 $cm^{-1}$ (the G band) assigned to MWCNTs tangential vibrations and the other one at 1331 $cm^{-1}$ (the D band) corresponding to the disorder mode introduced in the C $sp^2$ electronic structure by other types of atoms [27]. The $I_D/I_G$ ratio between the intensities of the two bands may give significant information about the non-covalent/covalent functionalization of the MWCNTs (Table 1). Thus it can be observed that the $I_D/I_G$ ratio increases after non-covalent treatment, which is a proof that the attachment of surfactants molecules has really occurred.

Similar Raman spectra were recorded also for the covalently functionalized MWCNTs. As it was expected by oxidation (MWCNT-COOH) the $I_D/I_G$ ratio increases in comparison with unmodified MWCNT, and this ratio further increased after covalent treatment. By comparing the data from Table 1 one may notice that the $I_D/I_G$ ratio is always higher for covalent treatment in comparison with the non-covalent procedure which may be explained by the fact that in the case of the covalent treatment the non-covalent attachment of surfactants molecules simultaneously occurs and therefore the disorder in the MWCNTs structures is increased.

**Table 1**
Raman data for D and G peaks of non-covalent functionalized MWCNTs.

| Nanotubes type | $I_G$ | $X_G$ ($cm^{-1}$) | $I_D$ | $X_D$ ($cm^{-1}$) | $\frac{I_D}{I_G}$ |
|---|---|---|---|---|---|
| MWCNT | 25.9 | 1581.5 | 39.1 | 1319.3 | 1.51 |
| MWCNT-SP135 | 24.8 | 1577.7 | 40.4 | 1319.3 | 1.63 |
| MWCNT-X100 | 17.0 | 1581.5 | 28.1 | 1323.1 | 1.65 |
| MWCNT-NP9 | 14.4 | 1593.1 | 25.1 | 1323.1 | 1.74 |
| MWCNT-COOH | 30.5 | 1589.2 | 49.4 | 1326.9 | 1.62 |
| MWCNT-COO-SP135 | 32.0 | 1573.8 | 54.7 | 1323.1 | 1.71 |
| MWCNT-COO-X100 | 63.7 | 1581.5 | 111.5 | 1323.1 | 1.75 |
| MWCNT-COO-NP9 | 40.6 | 1573.8 | 74.4 | 1319.3 | 1.83 |

The Raman data regarding the position of the two characteristic peaks are in accordance with the functionalization degree obtained from the $I_D/I_G$ ratio [28]. Comparing the unmodified MWCNTs with the functionalized ones it can be noticed that the highest shift of the D band occurred if NP9 was used as modifier both for the covalent and non-covalent functionalization methods, the large number of NP9 molecules attached to the MWCNTs surface being

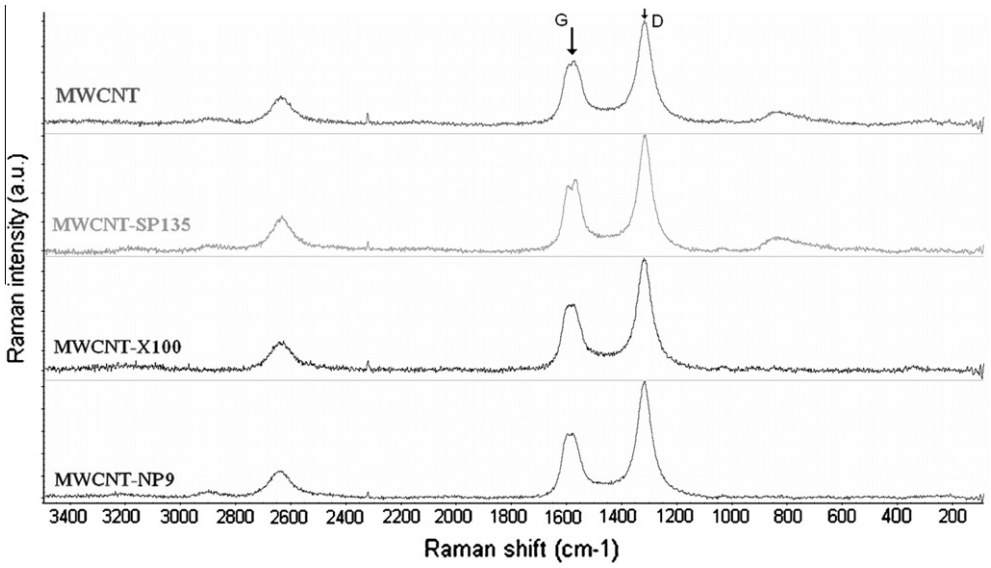


**Fig. 5.** Raman spectra for non-covalent functionalized MWCNTs compared with pristine MWCNTs.

responsible for the modification of the MWCNTs electronic structure.

XPS was used to examine the nature of surface species from the MWCNT before and after the functionalization. The asymmetric C1s spectra (Fig. 6) of pristine and non-covalent functionalized MWCNTs were deconvoluted using Gaussian–Lorentzian function centered at 284.6 eV corresponding to the C—C binding energy from internal reference and adding other symmetric Gaussian peaks, in accordance with the contributions from graphite-like walls and the carbon atoms from the attached molecules. The peak at approximately 285.5 eV is assigned to $sp^3$ C atoms from structural defects. For the pristine MWCNTs it can be observed the peak at 287.6 eV assigned to C═O species formed through the synthesis of MWCNTs. Also the usually peak at 291.0 eV assigned to $\pi$-$\pi^*$ electronic transition is shown in all spectra of the unmodified/modified MWCNTs. The peaks at about 286.4 eV can be assigned to —C—O— (alcohol, ether) species from the attached molecules. A rough evaluation of the ratio of peak areas leads to the conclusion that almost 20% of the carbon atoms from the analyzed surface were linked to oxygen atoms which is in good agreement with the optimal functionalization degree reported in the literature [29]. These results prove that MWCNTs can be modified by non-covalent attachment of surfactant molecules based on their van der Waals attraction forces, the oxygenous groups being detected on the side-walls, even after vigorous washing.

The comparison between the XPS spectra for the C 1s core levels of covalently functionalized MWCNTs and the XPS spectrum for the C 1s core level of MWCNT-COOH (Fig. 7) shows that the esterification reaction took place. Thus the C1s core level of the oxidized MWCNTs (Fig. 7a) could be deconvoluted to four fractional peaks with the binding energies at 284.6, 285.5, 289 and 291.9 eV. The main peak at 284.6 eV was attributed to $sp^2$ graphite-like C atoms, whereas the peak at 285.5 eV was assigned to $sp^3$ C atoms from the defects introduced by oxidation which is in good agreement with other data reported [30]. The peak at 289 eV corresponds to C atoms bonded to two O atoms (e.g., ester, carboxylic acid) [31,32]. Finally, the electronic $\pi$–$\pi^*$ transition peak was detected at approximately 291.9 eV [30]. The C 1s core level XPS spectra of MWCNT-COOH and modified MWCNTs show the presence of these four peaks, however in the case of modified MWCNTs with surfactants a new peak at ~286.7 eV was detected which was assigned to C atoms from C—O—C groups. This is a supplementary proof that the esterification really took place at the COOH groups from the MWCNT surface.

TEM images show the morphology of the functionalized MWCNTs compared with the pristine ones (Fig. 8). Thus it can be

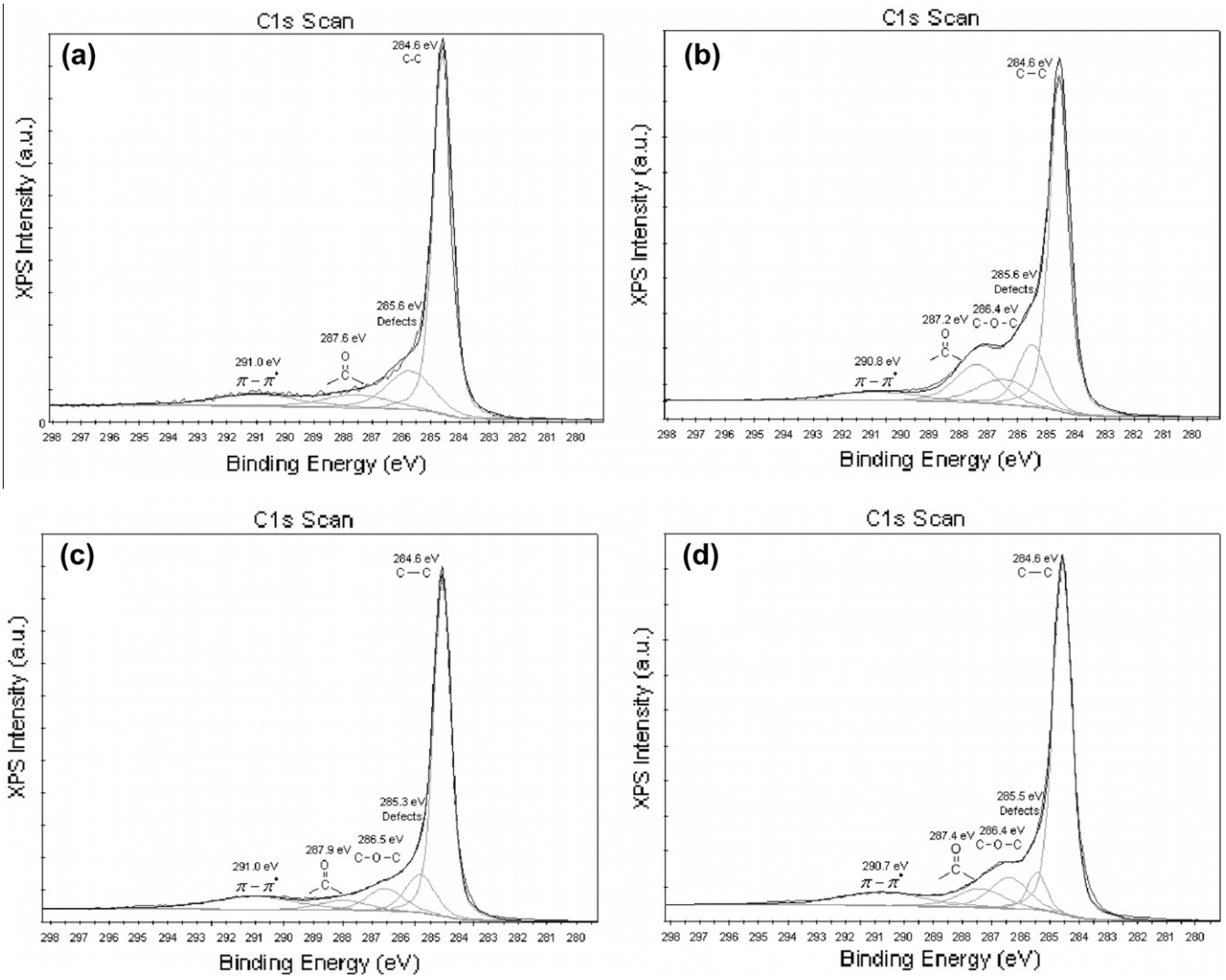


**Fig. 6.** XPS high resolution C1s spectra for: (a) MWCNT, (b) MWCNT-SP135, (c) MWCNT-X100, and (d) MWCNT-NP9.

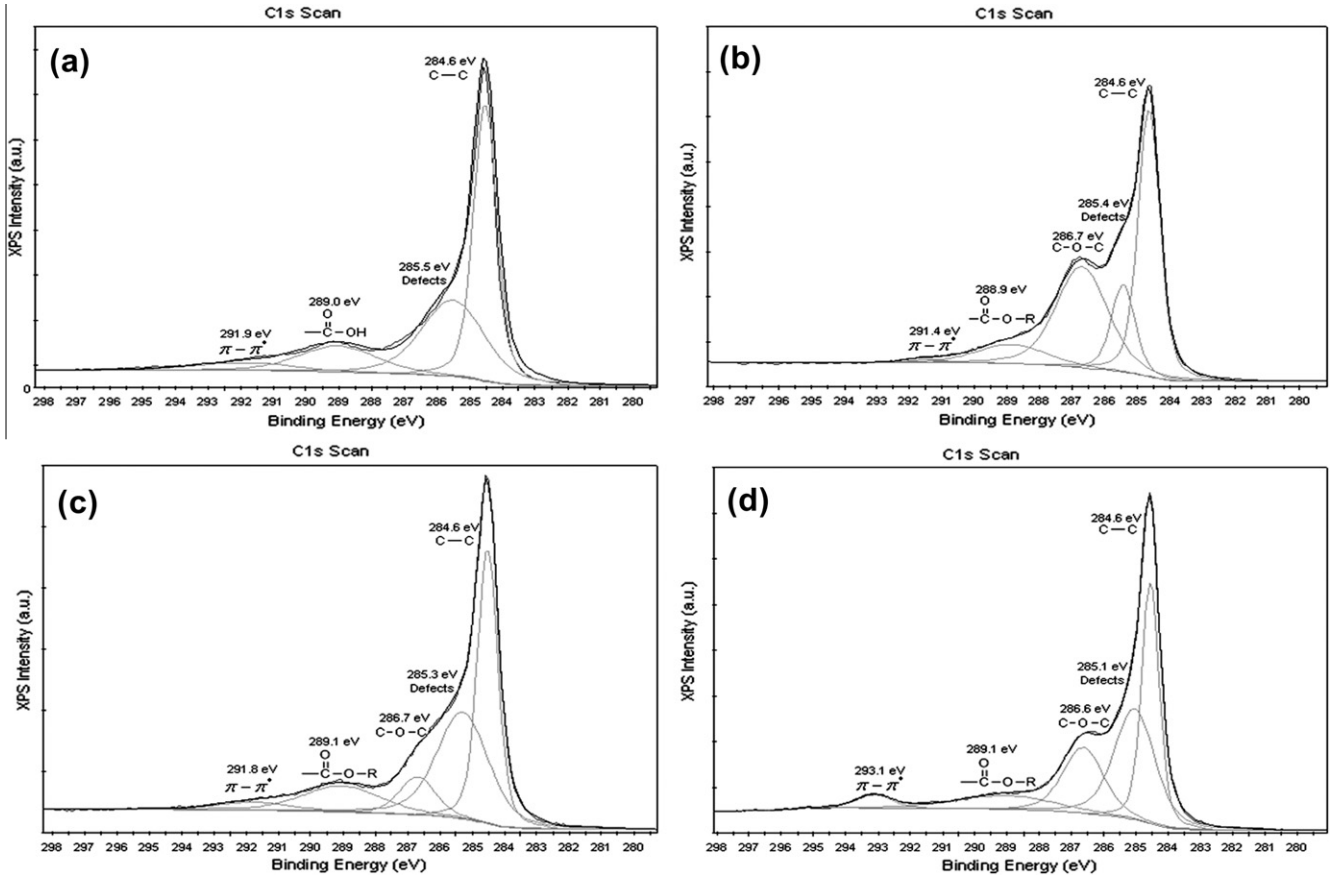


**Fig. 7.** XPS high resolution spectra of: (a) MWCNT-COOH, (b) MWCNT-COO-SP135, (c) MWCNT-COO-X100, and (d) MWCNT-COO-NP9.

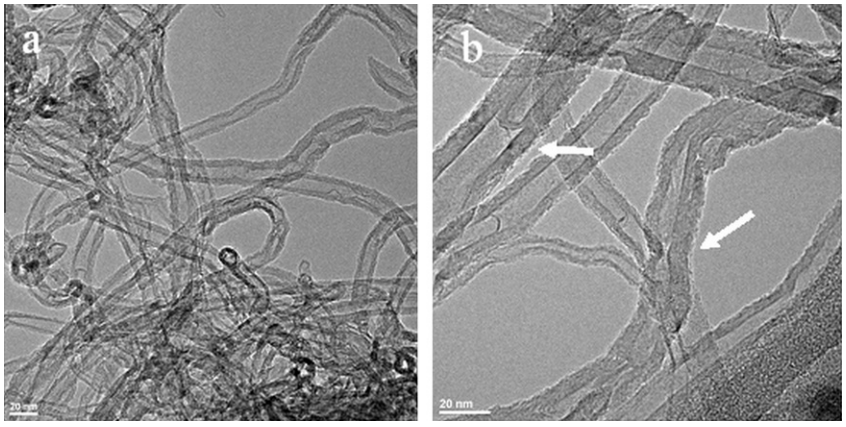


**Fig. 8.** TEM images for: (a) MWCNT and (b) MWCNT-SP135.

noticed that the pristine MWCNTs exhibit sharp edges, crystalline walls and smaller diameters compared with MWCNT-SP135 which show an amorphous layer surrounding the graphitic walls formed by the surfactants molecules. This layer will help to reduce the interfacial tension between the MWCNTs and the polymer matrix in a polymer-based composite material.

### 3.2. Epoxy composites characterization

From TGA data showed in Table 2 one can notice a lower thermostability of the composites reinforced with 1% pristine MWCNTs, probably caused by a low compatibility between the polymer matrix (DGEBA) and MWCNT, the latter forming aggregates within the polymer matrix. The incorporation of non-covalently functionalized MWCNTs has increased the thermostability by 7–9 °C, the functionalized MWCNTs being better dispersed. The highest values for the thermostability of the composites reinforced with both non-covalent and covalent functionalized MWCNTs were noticed in the case of SP135 surfactant although the functionalization degree calculated from Raman data was higher for the NP9. This is probably due to the longer aliphatic chain of SP135 which being more flexible may easily form hydrogen bonds with the DGEBA matrix.

For the covalently functionalized MWCNTs the TGA data from Table 2 shows a slight improvement of the 3% decomposition temperature of the corresponding epoxy nanocomposites. As it was ex-

**Table 2**
TGA data for the composite reinforced with non-covalently and covalently functionalized MWCNTs.

| Composite sample | Reinforcing agent (%) | $T_{d3\%}$ (°C) | $T_{d5\%}$ (°C) |
|---|---|---|---|
| DGEBA_PXDED | 0 | 327.0 | 337.9 |
| DGEBA_MWCNT_PXDED | 1 | 325.9 | 333.9 |
| DGEBA_MWCNT-SP135_PXDED | 1 | 335.5 | 342.5 |
| DGEBA_MWCNT-X100_PXDED | 1 | 333.0 | 341.6 |
| DGEBA_MWCNT-NP9_PXDED | 1 | 329.3 | 337.3 |
| DGEBA_MWCNT-COOH_PXDED | 1 | 333.4 | 340.9 |
| DGEBA_MWCNT-COO-SP135_PXDED | 1 | 339.3 | 346.2 |
| DGEBA_MWCNT-COO-X100_PXDED | 1 | 333.9 | 342.9 |
| DGEBA_MWCNT-COO-NP9_PXDED | 1 | 333.1 | 341.5 |

**Table 3**
DSC data for the composites reinforced with NP9 functionalized MWCNTs by both methods.

| Samples | $\Delta H$ (J/g) | $T_{max}$ (°C) |
|---|---|---|
| DGEBA_PXDED | 405 | 103 |
| DGEBA_MWCNT(1%)_PXDED | 411 | 107 |
| DGEBA_MWCNT-NP9(1%)_PXDED | 428 | 106 |
| DGEBA_MWCNT-COOH(1%)_PXDED | 420 | 106 |
| DGEBA_MWCNT-COO-NP9(1%)_PXDED | 433 | 105 |

**Table 4**
The $T_g$ values of the composites with non-covalent and covalent functionalized MWCNTs.

| Composite sample | Reinforcing agent (%) | $T_g$, °C at 1 Hz |
|---|---|---|
| DGEBA_PXDED | 0 | 119.9 |
| DGEBA_MWCNT_PXDED | 1 | 119.2 |
| DGEBA_MWCNT-SP135_PXDED | 1 | 121.5 |
| DGEBA_MWCNT-X100_PXDED | 1 | 119.9 |
| DGEBA_MWCNT-NP9_PXDED | 1 | 123.4 |
| DGEBA_MWCNT-COOH_PXDED | 1 | 127.8 |
| DGEBA_MWCNT-COO-SP135_PXDED | 1 | 122.6 |
| DGEBA_MWCNT-COO-X100_PXDED | 1 | 119.3 |
| DGEBA_MWCNT-COO-NP9_PXDED | 1 | 123.6 |

pected the increase of $T_{d3\%}$ and $T_{d5\%}$ values is much significant for the covalently functionalized MWCNTs than for the non-covalent ones which means that the covalent bonding of surfactant molecules onto the MWCNT surface leads to an increased dispersibility within the polymer matrix.

The DSC curves recorded for the curing reaction of epoxy-based composites reinforced with covalently functionalized MWCNTs (Fig. 9) show a slight shift of the maximum curing temperature to higher values, meaning that there are still some aggregated MWCNTs which hinder the curing agent molecules to reach the epoxy groups of the polymer matrix.

For both composites with non-covalently or covalently functionalized MWCNTs the maximum curing temperature is almost the same but the corresponding enthalpies are different as it can be seen from Table 3. Thus higher enthalpies are assigned to the curing process of polymer-based composites with covalently functionalized MWCNTs meaning that the covalently bonded surfactant molecules help more to improve the dispersibility of MWCNTs within the polymer matrix, this being in good agreement with TGA data.

The values of glass transition temperature ($T_g$) were determined from tan δ versus temperature curves and shown in Table 4. It may be observed that the $T_g$ values are quite the same for the DGEBA based composite and for those reinforced with unmodified MWCNTs and X100-functionalized MWCNTs regardless of the type of functionalization, covalent or non-covalent. An increased $T_g$ value was obtained for DGEBA-based composites reinforced with functionalized MWCNTs with SP135 and NP9 surfactants. This is due to the higher flexibility of SP135 chains which leads to a high number of hydrogen bonds with the polymer matrix. In the case of NP9 the higher functionalization degree as showed by Raman spectra is the key factor to obtain a better dispersibility of the MWCNTs and thus an increased interface area between the polymer matrix and the functionalized MWCNTs.

MWCNTs act as effective nanosize reinforcing agents if there are no aggregates with size higher than 5 μm in the final nanocomposite materials, otherwise the voids that are created would act as crack initiation sites [33]. Therefore the particles should be homogeneously distributed within the polymer matrix. It is important for the particles to debond in order to assume the strain applied on the polymer matrix. The data of compressive stress test of the composites reinforced with non-covalently modified MWCNTs are shown in Fig. 10. An improvement of the compressive stress at failure with 22% was observed if 1% of MWCNT-NP9 was used as reinforcing agent showing that the higher functionalization degree influences the final mechanical properties of composites by

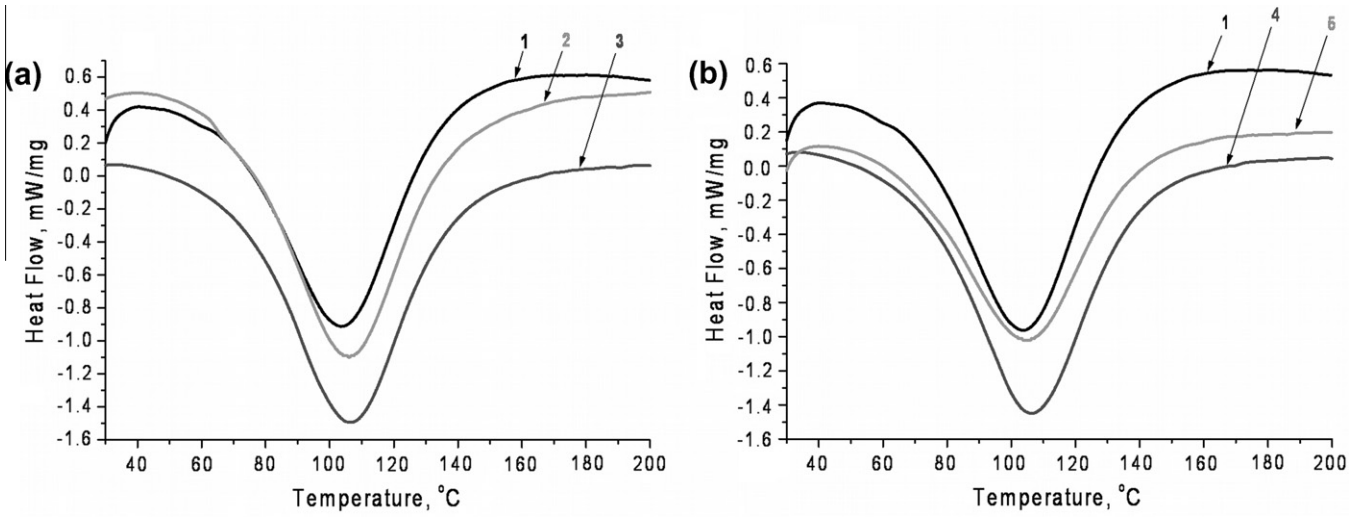


**Fig. 9.** DSC curves for the neat DGEBA (1) the composites with 1% MWCNT (2), MWCNT-NP9 (3) in *a* and the composites with MWCNT-COOH (4), MWCNT-COO-NP9 (5) in *b*.

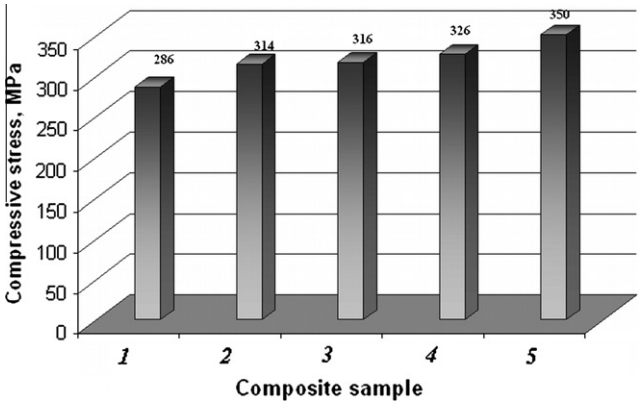


**Fig. 10.** Compression data for the neat DGEBA (1) and the composites reinforced with 1% MWCNT (2), MWCNT-SP135 (3), MWCNT-X100 (4) and MWCNT-NP9 (5).

creating an anisotropic material with individual CNTs in all directions which take over the load from the polymeric matrix as mentioned also by Sahoo et al. [34].

The fractured surfaces of the MWCNT/epoxy composites show a good dispersion of the functionalized MWCNTs with NP9 surfactant within the epoxy matrix and also a good adhesion of the polymer matrix to NP9-functionalized MWCNT surface compared with MWCNT-SP135 and especially MWCNT-X100 which have been pulled out from the matrix during the preparing method by fracturing of composites (Fig. 11). A large number of broken ends of the nanotubes can be seen on the fracture surface revealing that the dispersion of functionalized MWCNTs within the epoxy matrix was improved trough functionalization with surfactants.

As it can be observed from Fig. 12a–c, all the surfactant functionalized MWCNTs exhibit a good dispersibility in the epoxy matrix and therefore a high dispersion degree within the epoxy matrix was achieved by sonication with very few agglomerates still remained. This is due to the increased compatibility of the MWCNTs with the polymer matrix given by the functional groups and the possible hydrogen bonding of their hydroxyl groups with the ones from epoxy resin. Fig. 12c shows a very good polymer adhesion to the MWCNT-NP9. Some of the imaged MWCNTs are coming out of the prepared films plane. These MWCNTs have not been cut by the diamond blade but pulled out. However the MWCNTs are coated by an epoxy layer which indicates a very strong polymer adhesion.

## 4. Conclusions

The functionalization of MWCNTs with three types of surfactants based on aromatic and aliphatic polyglycols was done either covalently or non-covalently. It was successfully proved by TGA and FT-IR data and confirmed by Raman spectra showing that the highest functionalization degree was achieved using NP9 as modifier agent probably due to a higher compatibility between the structure of NP9 and the MWCNTs.

The XPS data also showed that the functionalization occurred considering the new deconvoluted peaks assigned to C—O—C groups from the surfactants in the case of non-covalent modification or those attributed to —COO— groups formed by the esterification reaction between the MWCNT-COOH and the surfactant in the case of covalent modification.

The covalently functionalized MWCNTs lead to a higher thermostability of the epoxy-based composites especially in the case of using SP135 surfactant which may easily form hydrogen bonds with the polymer matrix. Also the covalent modified MWCNTs increase the dispersibility within the polymer matrix.

The values of $T_g$ and compressive stresses at failure for epoxy-based composites reinforced with various modified MWCNTs showed that there are two main factors which strongly influence the final properties of these materials. The first one is the ability of the surfactant used to functionalize the MWCNTs to ensure their

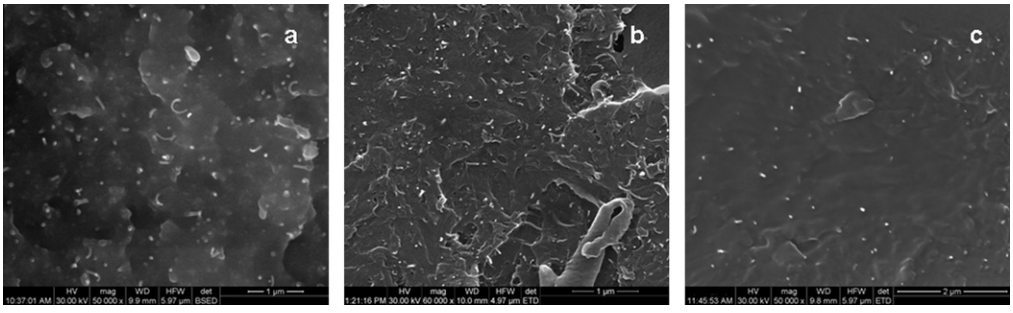


**Fig. 11.** SEM images for epoxy composites reinforced with 1 wt.%: (a) MWCNT-SP135, (b) MWCNT-X100, and (c) MWCNT-NP9.

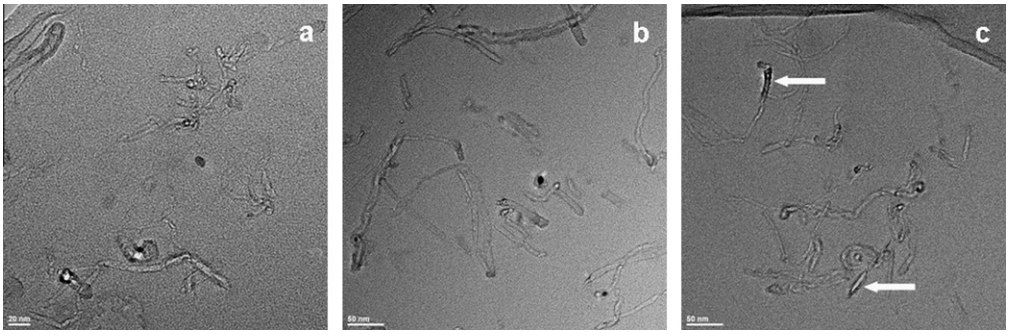


**Fig. 12.** TEM images for epoxy composites reinforced with 1 wt.%: (a) MWCNT-SP135, (b) MWCNT-X100, and (c) MWCNT-NP9.

good dispersion within the polymer matrix and the second one is the capacity of the surfactant to form eventually bonds with the polymer itself. A positive combination of these two factors, like in the case of SP135 surfactant leads to composites with improved properties.

## References


[1] Yang SY, Ma CCM, Teng CC, Huang YW, Liao SH, Huang YL, et al. Effect of functionalized carbon nanotubes on the thermal conductivity of epoxy composites. Carbon 2010;48:592–603.

[2] Jorge GA, Bekeris V, Escobar MM, Goyanes S, Zilli D, Cukierman AL, et al. A specific heat anomaly in multiwall carbon nanotubes as a possible sign of orientational order–disorder transition. Carbon 2010;48:525–30.

[3] Niu L, Luo Y, Li Z. A highly selective chemical gas sensor based on functionalization of multi-walled carbon nanotubes with poly(ethylene glycol). Sens Actuators B 2007;126:361–7.

[4] Wang D, Lu J, Zhou J, Lai L, Wang L, Luo G, et al. Selective adsorption of cations on single-walled carbon nanotubes: a density functional theory study. Comput Mater Sci 2008;43:886–91.

[5] Park JM, Kim DS, Kim SJ, Kim PG, Yoon DJ, DeVries KL. Inherent sensing and interfacial evaluation of carbon nanofiber and nanotube/epoxy composites using electrical resistance measurement and micromechanical technique. Composites Part B 2007;38:847–61.

[6] Datsyuk V, Landois P, Fitremann J, Peigney A, Galibert AM, Soula B, et al. Double-walled carbon nanotube dispersion via surfactant substitution. J Mater Chem 2009;19:2729–36.

[7] Martonea A, Formicolab C, Giordanob M, Zarrellib M. Reinforcement efficiency of multi-walled carbon nanotube/epoxy nano composites. Compos Sci Technol 2010;70(7):1154–60.

[8] Petrea CM, Gârea SA, Iovu H. The influence of different types of carbon nanotubes on the synthesis and properties of epoxy-based nanocomposite materials. Mater Plast 2008;45(1):34–7.

[9] Petrea CM, Andronescu C, Pandele AM, Gârea SA, Iovu H. Advanced characterization of modified carbon nanotubes epoxy-based composites. Mater Plast 2008;45(1):320–5.

[10] Visco A, Calabrese L, Milone C. Cure rate and mechanical properties of a dgebf epoxy resin modified with carbon nanotubes. J Reinf Plast Compos 2009;28(08):937–49.

[11] Thakre PR, Bisrat Y, Lagoudas DC. Electrical and mechanical properties of carbon nanotube-epoxy composites. J Appl Polym Sci 2010;116:191–202.

[12] Yu S, Tong MN, Critchlow G. Use of carbon nanotubes reinforced epoxy as adhesives to join aluminum plates. Mater Des 2010;31:S126–129.

[13] Titus E, Ali N, Cabral G, Gracio J, Ramesh Babu P, Jackson MJ. Chemically functionalized carbon nanotubes and their characterization using thermogravimetric analysis, fourier transform infrared, and raman spectroscopy. J Mater Eng Perform 2006;15:182–6.

[14] Zeng L, Alemany LB, Edwards CL, Barron AR. Demonstration of covalent sidewall functionalization of single wall carbon nanotubes by NMR spectroscopy: side chain length dependence on the observation of the sidewall sp3 carbons. Nano Res 2008;1:72–88.

[15] Chen H, Xiong H, Gao Y, Li H. Covalent functionalization of multiwalled carbon nanotubes with polybutadiene. J Appl Polym Sci 2010;116:1272–7.

[16] Manivannan S, Jeong IO, Ryu JH, Lee CS, Kim KS, Jang J, et al. Dispersion of single-walled carbon nanotubes in aqueous and organic solvents through a polymer wrapping functionalization. J Mater Sci: Mater Electron 2009;20:223–9.

[17] Xu L, Ye Z, Cui Q, Gu Z. Noncovalent nonspecific functionalization and solubilization of multi-walled carbon nanotubes at high concentrations with a hyperbranched polyethylene. Macromol Chem Phys 2009;210:2194–202.

[18] Petrea CM, Andronescu C, Pandele AM, Garea SA, Iovu H. Epoxy-based composites with amine modified single walled carbon nanotubes. E-Polymers; 2010. 020.

[19] Damian CM, Pandele AM, Andronescu C, Ghebaur A, Garea SA, Iovu H. Epoxy-based composites reinforced with new amino functionalized multi-walled carbon nanotubes. Fuller Nanotub Car N 2011;19(3):197–209.

[20] Liu X, Chan-Park MB. Facile way to disperse single-walled carbon nanotubes using a noncovalent method and their reinforcing effect in poly(methyl methacrylate) composites. J Appl Polym Sci 2009;114:3414–9.

[21] Bredeau S, Peeterbroeck S, Bondue D, Alexandre M, Dubois P. From carbon nanotube coatings to high-performance polymer composites. Polym Int 2008;57:547–53.

[22] Vaisman L, Wagner HD, Marom G. The role of surfactants in dispersion of carbon nanotubes. Adv Colloid Interface Sci 2006;128–130:37–46.

[23] Anson-Casaos A, Gonzalez-Dominguez JM, Martinez MT. Separation of single-walled carbon nanotubes from graphite by centrifugation in a surfactant or in polymer solutions. Carbon 2010;48:2917–24.

[24] Bystrzejewski M, Huczko A, Lange H, Gemming T, Büchner B, Rümmeli MH. Dispersion and diameter separation of multi-wall carbon nanotubes in aqueous solutions. J Colloid Interface Sci 2010;345:138–42.

[25] Rausch J, Zhuang RC, Mäder E. Surfactant assisted dispersion of functionalized multi-walled carbon nanotubes in aqueous media. Compos Part A – Appl Sci 2010;41:1038–46.

[26] Hong CE, Lee JH, Kalappa P, Advani SG. Effects of oxidative conditions on properties of multi-walled carbon nanotubes in polymer composites. Compos Sci Technol 2007;67:1027–34.

[27] Dresselhaus MS, Dresselhaus G, Saito R, Jorio A. Raman spectroscopy of carbon nanotubes. Phys Rep 2005;409(2):47–99.

[28] Delhaes P, Couzi M, Trinquecoste M, Dentzer J, Hamidou H, Vix-Guterl C. A comparison between Raman spectroscopy and surface characterizations of multiwall carbon nanotubes. Carbon 2006;44:3005–13.

[29] Yu H, Jin Y, Peng F, Wang H, Yang J. Kinetically controlled side-wall functionalization of carbon nanotubes by nitric acid oxidation. J Phys Chem C 2008;112(17):6758–63.

[30] Yang K, Gu M, Guo Y, Pan X, Mu G. Effects of carbon nanotube functionalization on the mechanical and thermal properties of epoxy composites. Carbon 2009;47:1723–37.

[31] Clark MD, Subramanian S, Krishnamoorti R. Understanding surfactant aided aqueous dispersion of multi-walled carbon nanotubes. J Colloid Interface Sci 2011;354:144–51.

[32] Lee GW, Kim J, Yoon J, Bae JS, Shin BC, Kim IS, et al. Structural characterization of carboxylated multi-walled carbon nanotubes. Thin Solid Films 2008;516:5781–4.

[33] Tjong SC. Structural and mechanical properties of polymer composites. Mater Sci Eng R 2006;53:73–197.

[34] Sahoo NG, Cheng HKF, Li L, Chan SH, Judeh Z, Zhao J. Specific functionalization of carbon nanotubes for advanced polymer composites. Adv Funct Mater 2009;19:1–10.